

Dynamic charge inhomogeneity in cuprate superconductors

Thomas Bauer, Claus Falter

E-mail: falter@uni-muenster.de

Institut für Festkörperteorie, Westfälische Wilhelms-Universität,
Wilhelm-Klemm-Str. 10, 48149 Münster, Germany

Abstract. The inelastic x-ray scattering spectrum for phonons of Δ_1 -symmetry including the CuO bond-stretching phonon dispersion is analyzed by a Lorentz fit in $\text{HgBa}_2\text{CuO}_4$ and $\text{Bi}_2\text{Sr}_2\text{CuO}_6$, respectively, using recently calculated phonon frequencies as input parameters. The resulting mode frequencies of the fit are almost all in good agreement with the calculated data. An exception is the second highest Δ_1 -branch comprising the bond-stretching modes which disagrees in both compounds with the calculations. This branch unlike the calculations shows an anomalous softening with a minimum around the wavevector $\mathbf{q} = \frac{2\pi}{a}(0.25, 0, 0)$. Such a disparity with the calculated results, that are based on the assumption of an undisturbed translation- and point group invariant electronic structure of the CuO plane, indicates some *static* charge inhomogeneities in the measured probes. Most likely these will be charge stripes along the CuO bonds which have the strongest coupling to certain longitudinal bond-stretching modes that in turn selfconsistently induce corresponding *dynamic* charge inhomogeneities. The symmetry breaking by the mix of dynamic and static charge inhomogeneities can lead to a reconstruction of the Fermi surface into small pockets.

PACS numbers: 74.25.Kc, 74.72.Gh, 63.20.dd, 63.10.+a

In recent work [1, 2] the IXS phonon spectrum of optimally doped $\text{HgBa}_2\text{CuO}_4$ and $\text{Bi}_2\text{Sr}_2\text{CuO}_6$, respectively, has been measured for the Δ_1 -symmetry modes. The spectra have been interpreted by a Voigt fit function. For the interesting high frequency part of the spectra where the CuO bond-stretching modes (BSM) are expected that are known to display an anomalous softening upon doping in the cuprates [3, 4, 5, 6, 7, 8, 9, 10, 11, 12], only one phonon peak has been fitted in case of $\text{HgBa}_2\text{CuO}_4$ [1] and two in case of $\text{Bi}_2\text{Sr}_2\text{CuO}_6$ [2].

On the other hand, from our microscopic calculation of the phonon dynamics of $\text{HgBa}_2\text{CuO}_4$ and $\text{Bi}_2\text{Sr}_2\text{CuO}_6$ [13] we find in the high energy region of the IXS spectra along $\frac{2\pi}{a}(\zeta, 0, 0)$ up to four Δ_1 modes as far as $\text{HgBa}_2\text{CuO}_4$ is concerned and up to five Δ_1 modes in $\text{Bi}_2\text{Sr}_2\text{CuO}_6$. These modes interact strongly with each other and constitute a highly nontrivial anticrossing scenario. As a consequence a multiple mode fit is necessary to obtain more reliable results. The strength of the measured peaks strongly decreases for larger ζ values such that at $\zeta \approx 0.5$ the peaks are very weak, see e.g. figure 1, and an unique interpretation taking only one or two peaks into account is incomplete because of the many modes of the same symmetry in this region of energy. Nevertheless, it is very interesting that in the limited Voigt fit of the spectra in [1, 2] a hint to an anomalous softening of the BSM-dispersion is extracted at $\zeta \approx 0.3$ in the Hg compound and at $\zeta \approx 0.25$ in the Bi compound. Such an enhanced softening at these ζ values has not been detected in our calculations for the Δ_1 modes. Only the presumably generic softening in the cuprates of the half-breathing mode (HBM) in $\text{HgBa}_2\text{CuO}_4$ and of two half-breathing modes in $\text{Bi}_2\text{Sr}_2\text{CuO}_6$, generated by the strong nonlocal electron-phonon interaction (EPI) mediated by the charge fluctuations (CF) on the outer electron shells of the ions, has been found in our calculations [13].

In the presence of these theoretical results and the complex anticrossing of the Δ_1 modes it is very desirable to perform a more complete analysis of the IXS measurements on the basis of the calculation of the dispersion of the Δ_1 modes as given in [13]. In such a reconstruction of the IXS phonon spectra we do not apply the more complicated Voigt fit but use instead a more simple Lorentz fit function, which does the job very well. This can be concluded from figure 1 (a) where the IXS spectrum of $\text{HgBa}_2\text{CuO}_4$ [1] is reconstructed for $\mathbf{q} = \frac{2\pi}{a}(\zeta, 0, 0)$ using as in [1] only one peak in the Lorentz fit. The phonon frequencies fitted at $\zeta = 0.11, 0.17, 0.23, 0.29, 0.36, 0.42$ and 0.48 are 16.28 (16.32), 15.76 (15.73), 14.61 (14.65), 13.38 (13.73), 13.15 (13.14), 13.40 (13.53) and 13.51 (13.63) THz. The data within the brackets are the frequencies as obtained from the Voigt fit [1]. We recognize a very good agreement between both fitting procedures. As far as $\text{Bi}_2\text{Sr}_2\text{CuO}_6$ is concerned we also get nearly undistinguishable results for a two mode fit in the two fitting schemes, so we take the more simple Lorentz fit in this work.

In figure 1 (b) we present the results of the Lorentz fit for the analysis the IXS spectrum of $\text{HgBa}_2\text{CuO}_4$ within the framework of the calculated Δ_1 -modes in the relevant energy range [13]. As already mentioned up to four mode frequencies must be considered. The calculated frequencies at the corresponding ζ values are taken as input parameters of the Lorentz fit. From the results displayed in figure 1 (b) we find

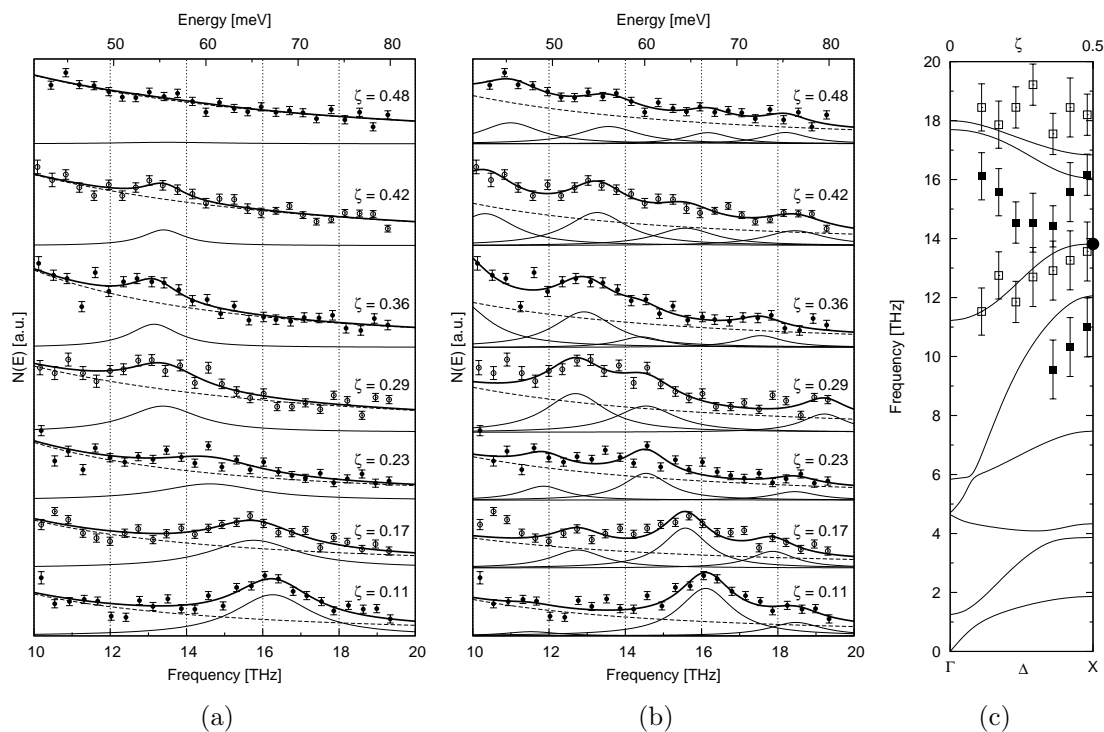


Figure 1. (a) Reconstructed IXS phonon spectrum of $\text{HgBa}_2\text{CuO}_4$ from [1] for $\mathbf{q} = \frac{2\pi}{a}(\zeta, 0, 0)$ using a Lorentz fit with one mode only (thick line), the corresponding Lorentz peaks of the modes are also shown (thin line). The broken line represents the elastic background. The inelastic cross section $N(E)$ is given in arbitrary units. (b) Same as in (a) but using a Lorentz fit on the basis of the calculated phonon dispersion for modes of Δ_1 -symmetry in the energy range considered [13]. (c) Calculated phonon dispersion of $\text{HgBa}_2\text{CuO}_4$ for modes of Δ_1 -symmetry according to [13]. The symbols \blacksquare and \square denote the phonon frequencies from the Lorentz fit and \bullet the half-breathing mode. The vertical bars indicate the FWHM of the peaks determined in the fitting.

that the IXS spectrum is well represented by the multiple mode fit. The Lorentz peaks as obtained by the fit are also shown in the figure for each ζ value.

The resulting phonon frequencies from the fit are shown in figure 1 (c) together with the calculated dispersion of the Δ_1 modes [13]. With exception of the second highest Δ_1 branch comprising the BSM that displays the anomalous softening starting at $\zeta \approx \frac{1}{8}$ with a minimum around $\zeta = \frac{1}{4}$, the resulting mode frequencies are in reasonable agreement with the calculated branches.

In case of $\text{Bi}_2\text{Sr}_2\text{CuO}_6$ the Lorentz fit of the IXS spectrum on the basis of the calculated Δ_1 -modes [13] is shown in figure 2 (b) and likewise as in $\text{HgBa}_2\text{CuO}_4$ a good resolution of the spectrum is achieved. The extracted phonon frequencies from the fit are shown in figure 2 (c). For a comparison the calculated dispersion of the Δ_1 -modes [13] are displayed in the figure. Leaving aside the second highest branch we find a good agreement of the calculated branches with the modes from the Lorentz fit. As for $\text{HgBa}_2\text{CuO}_4$ the second highest Δ_1 branch displays an anomalous softening starting at $\zeta \approx \frac{1}{8}$ with a minimum around $\zeta = \frac{1}{4}$.

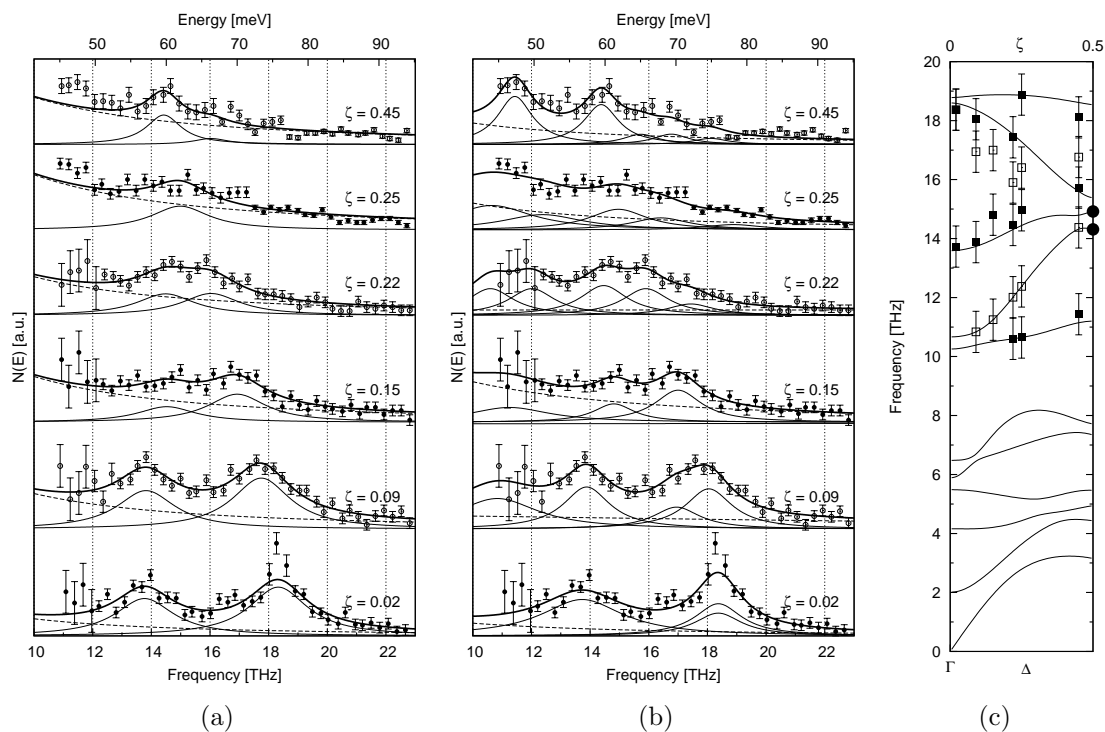


Figure 2. (a) Reconstructed IXS phonon spectrum of $\text{Bi}_2\text{Sr}_2\text{CuO}_6$ from [2] for $\mathbf{q} = \frac{2\pi}{a}(\zeta, 0, 0)$ using a Lorentz fit with two modes only (thick line), the corresponding Lorentz peaks of the modes are also shown (thin line). The broken line represents the elastic background. The inelastic cross section $N(E)$ is given in arbitrary units. (b) Same as in (a) but using a Lorentz fit on the basis of the calculated phonon dispersion for modes of Δ_1 -symmetry in the energy range considered [13]. (c) Calculated phonon dispersion of $\text{Bi}_2\text{Sr}_2\text{Cu}_6$ for modes of Δ_1 -symmetry according to [13]. The symbols \blacksquare and \square denote the phonon frequencies from the Lorentz fit and \bullet the half-breathing modes. The vertical bars indicate the FWHM of the peaks determined in the fitting.

Strong coupling of the BSM with dynamic charge stripes generated selfconsistently via strong nonlocal electron-phonon interaction (EPI) by the BSM themselves leading to an anomalous softening has already been found earlier in the cuprate based superconductors for the case of an undisturbed translation- and point group invariant electronic structure of the CuO plane without any charge inhomogeneities [14, 15, 16, 17, 18, 19]. The same holds true for $\text{HgBa}_2\text{CuO}_4$ and $\text{Bi}_2\text{Sr}_2\text{CuO}_6$ as can be seen from the calculations in this work displayed in figure 3, where the charge redistribution $\delta\rho(\mathbf{r})$ for the half-breathing mode (HBM) ($\zeta = \frac{1}{2}$) induced by nonlocal EPI is shown. In the HBM propagating in $\Delta \sim (1, 0, 0)$ direction the O_x ions move coherently along the CuO bond towards or away from the silent Cu ion. For the detailed displacement pattern, see [13].

Figure 3 illustrates that the HBM creates in both compounds dynamic charge ordering $\delta\rho$ via charge fluctuations at the ions due to nonlocal EPI in form of localized stripes of alternating sign in the CuO plane. The period of the pattern is twice the lattice constant for $\zeta = \frac{1}{2}$. In case of $\text{Bi}_2\text{Sr}_2\text{CuO}_6$ these dynamic charge inhomogeneities

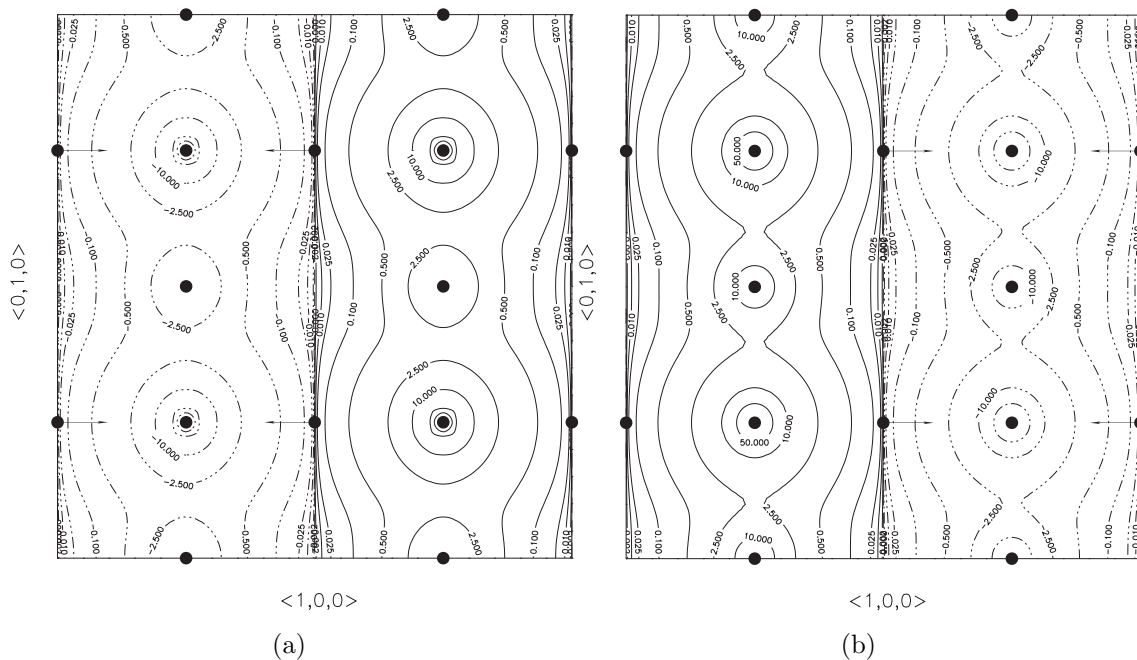


Figure 3. Dynamical charge stripes $\delta\rho$ as induced by the half-breathing mode (with the lower frequency) in $\text{Bi}_2\text{Sr}_2\text{CuO}_6$ (a) and in $\text{HgBa}_2\text{CuO}_4$ (b). The arrows indicate the vibrating oxygen ions. Units are in $10^{-4} e^2/a_B$. Regions of space where electrons are accumulated are characterized by full lines and those where electrons are pushed away by broken-dotted lines.

are only shown for one of the two HBM modes found in the calculations namely the one with the lower frequency, see figure 2 (c), because the charge redistribution is very similar for the other HBM. For $\text{HgBa}_2\text{CuO}_4$ we obtain only one HBM, see figure 1 (c), which induces the dynamic stripe pattern in figure 3 (b). In the HBM the dynamic charge stripes point along the x - or y -axis, respectively, if the oxygen ions move along the CuO bond in y - or x -direction, respectively.

It should be noted that for the oxygen breathing mode at the X point, see [13], the dynamic stripes excited point along the diagonals of the CuO plane. Furthermore, it should be remarked that dynamic charge inhomogeneities like the dynamic stripe patterns would not be present in systems with only *local* EPI at work. For example in a high density homogeneous electron gas prevailing in simple metals. This is because of perfect screening of the changes of the Coulomb potential related to the displacement of the ions in a phonon mode. On the other hand, our calculations exhibit a strong nonlocal EPI in the cuprates essentially due to the poor screening in these materials with a large component of ionic binding, see. e.g. [19]. This fact demonstrates the special role of a strong nonlocal EPI for the physics of these compounds in their normal as well as in the superconducting state.

Such a strong coupling is also underlined by recent experimental results for the quasi-particle dispersion in $(\text{Bi,Pb})_2\text{Sr}_2\text{CuO}_{6+\delta}$ [20]. The super-high resolution laser-based angle-resolved photoemission spectroscopy measurements reported in [20] show

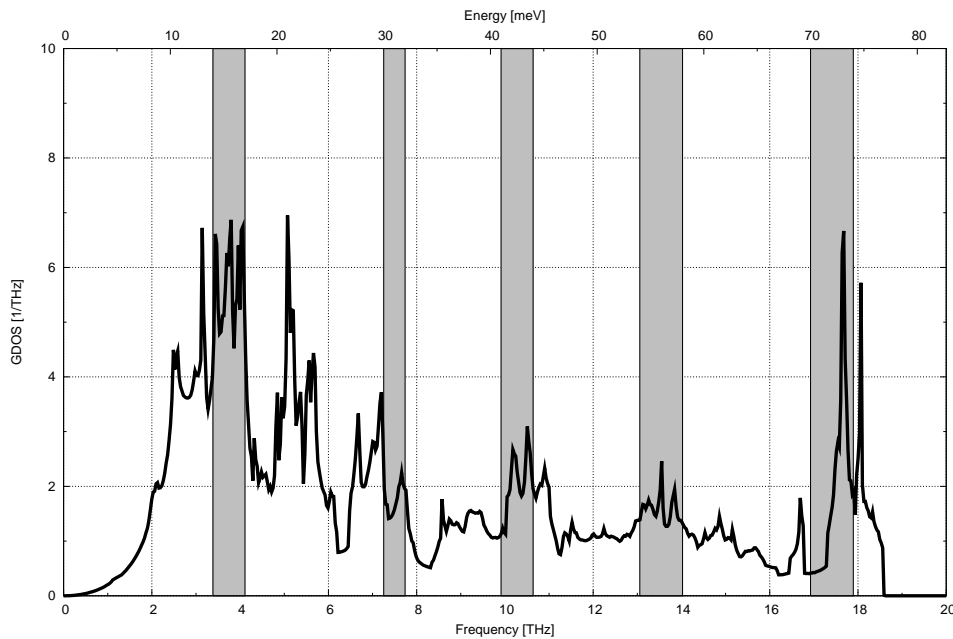


Figure 4. Calculated phonon density of states for $\text{Bi}_2\text{Sr}_2\text{CuO}_6$. The gray domains mark the peaks of the Eliashberg spectral function [20].

unambiguously that the ~ 70 meV nodal kink in the dispersion is due to strong EPI with multiple phonon modes as seen in the Eliashberg spectral function extracted from the measured real part of the electron self-energy. Remarkably, the peak structure of the Eliashberg function is in very good agreement with our calculated phonon density of states for $\text{Bi}_2\text{Sr}_2\text{CuO}_6$ [13], see figure 4.

Quite generally, our calculations for the cuprates demonstrate the enhanced susceptibility of the BSM for inducing dynamic charge inhomogeneities in form of stripes in the CuO plane. So, it can safely argued that the latter also will occur in a modified way in systems with static stripe charge order breaking translation- and point group invariance. The anomalous softening around $\zeta = \frac{1}{4}$ found by the analysis of the IXS phonon spectra then reflects the strong nonlocal coupling of the BSM with their selfconsistently induced dynamic charge inhomogeneities (dynamic stripes) but now in probes with a static charge inhomogeneity (static stripes) presumably present. Excess holes in a stripe will even enhance the strong nonlocal coupling to the BSM and consequently also the magnitudes of the CF's and the related mode softening is increased. An interrelation between the number of holes and softening is supported by the experiment and our calculations for the Cu-O-bond stretching modes [14, 15].

The symmetry breaking of the electronic structure by charge inhomogeneity in form of static stripe patterns accompanied by phonon-induced dynamic fluctuating patterns shown by our calculations to occur very likely may lead to a corresponding reconstruction of the Fermi surface into small pockets. This reconstruction is in turn the origin for the quantum oscillations measured in some cuprates, see e.g. [21]. In this context it is interesting, that in [22] the quantum oscillations are attributed to symmetry breaking

by a certain type of stripe order in form of a combined charge/ spin modulation. Other authors attribute the small Fermi surface pockets to magnetic fluctuations [23], to d -density wave [24] or to an antiferromagnetic (π, π) spin density wave [25].

Finally, it should be added that in the literature dynamic charge inhomogeneities related to electron-phonon coupling are discussed from the experimental side for $\text{La}_{2-x}\text{Ba}_x\text{CuO}_4$, $\text{YBa}_2\text{Cu}_3\text{O}_7$ or $\text{Ba}_{0.6}\text{K}_{0.4}\text{BiO}_3$ in [26, 27, 28, 29, 30, 31, 32, 33] and from the theoretical side e.g. in [34].

In summary, our analysis of the IXS phonon spectra for $\text{HgBa}_2\text{CuO}_4$ and $\text{Bi}_2\text{Sr}_2\text{CuO}_6$ within the framework of calculated phonon dispersion curves points to the existence of dynamic charge inhomogeneities generated by the BSM via strong nonlocal EPI of the CF-type. These modes excite dynamic charge order and consequently can also serve as indirect probes for corresponding static charge order in the cuprates. Thus, we have a mix of static and fluctuating charge order in the materials.

References

- [1] Uchiyama H et al 2004 Phys. Rev. Lett. **92** 197005
- [2] Graf J et al 2008 Phys. Rev. Lett. **100** 227002
- [3] Pintschovius L 2005 Phys. Status Solidi b **242** 30
- [4] Pintschovius L and Reichardt W 1998 *Neutron Scattering in Layered Copper-Oxide Superconductors (Physics and Chemistry of Materials with Low Dimensional Structures vol 20)* ed A Furrer (Dordrecht: Kluwer Academic)
- [5] Pintschovius L and Braden M 1999 Phys. Rev. B **60** R15039
- [6] Reichardt W 1996 J. Low. Temp. Phys. **105** 807
- [7] Fukuda T et al 2005 Phys. Rev. B **71** R060501
- [8] Pintschovius L et al 2006 Phys. Rev. B **74** 174514
- [9] McQueeney RJ et al 2001 Phys. Rev. Lett. **87** 077001
- [10] d'Astuto M et al 2002 Phys. Rev. Lett. **88** 167002
- [11] d'Astuto M et al 2003 Int. J. Mod. Phys. B **17** 484
- [12] Braden M et al 2005 Phys. Rev. B **72** 184517
- [13] Bauer T and Falter C 2010 J. Phys.: Condens. Matter **22** 055404
- [14] Falter C 2005 Phys. Status Solidi b **242** 78
- [15] Falter C, Bauer T and Schnetgöke F 2006 Phys. Rev. B **73** 224502
- [16] Falter C et al 1997 Phys. Rev. B **55** 3308
- [17] Bauer T and Falter C 2008 Phys. Rev. B **77** 144503
- [18] Falter C and Hoffmann G 2000 Phys. Rev. B **61** 14537
- [19] Bauer T and Falter C 2009 Phys. Rev. B **80** 094525
- [20] Zhao L et al 2010 arXiv:1002.0120
- [21] Doiron-Leyraud N et al 2007 Nature **447** 565
- [22] Taillefer L 2009 J.Phys.: Condens. Matter **21** 164212
- [23] Harrison N et al 2009 J.Phys.: Condens. Matter **21** 322202
- [24] Chakravarty S and Kee HY 2008 Proc. Natl. Acad. Sci. U.S.A. **105** 8835
- [25] Lin J and Millis AJ 2005 Phys. Rev. B **72** 214506
- [26] Reznik D et al Nature 2006 **440** 1170
- [27] d'Astuto M et al 2008 Phys. Rev. B **78** R140511
- [28] Pintschovius L et al 2004 Phys. Rev. B **69** 214506
- [29] McQueeney R J et al 1999 Phys. Rev. Lett. **82** 628
- [30] Pintschovius L et al 2003 arXiv:cond-mat/0308357

- [31] Chung JH et al 2003 Phys. Rev. B **67** 014517
- [32] Braden M et al 2001 arXiv:cond-mat/0107498
- [33] Braden M et al 2002 Physica C **378-381** 89
- [34] Kaneshita et al 2002 Phys. Rev. Lett. **88** 115501